

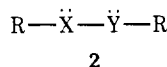
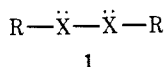
Lone Pair–Lone Pair Interactions in Unsymmetrical Systems: RSSR vs. RSOR¹

James P. Snyder*² and Lars Carlsen

Contribution from the Department of General and Organic Chemistry, University of Copenhagen, The H. C. Ørsted Institute, Universitetsparken 5, DK-2100 Copenhagen Ø, Denmark. Received August 9, 1976

Abstract: The conformational behavior of the symmetrical disulfide function, RSSR, and the unsymmetrical sulfenate ester moiety, RSOR (R = H, CH₃), have been compared by means of semiempirical MO calculations. Particular attention has been paid to the α -lone pair interactions. The two species are predicted to exhibit comparable equilibrium geometries and to undergo conformational transformation with qualitatively similar energy requirements. Where data are available, agreement with experiment is good to excellent. Comparison at the level of molecular orbital energy levels reveals that further resemblance between the RSSR and RSOR systems is absent. Orbital correlation diagrams for motion through the dihedral angle θ permit qualitative predictions concerning the relative photoelectron and UV spectra. The latter have been evaluated as a function of conformation in more detail by means of CNDO/S–CI calculations. The first absorption band relationship $\lambda_{\max}(\text{RSOR}) > \lambda_{\max}(\text{RSSR})$, inadequately described by single configuration schemes, is correctly predicted by the fuller treatment. Supplemental computations for three- and four-membered ring disulfides and sulfenate esters extend the results and suggest an interpretative guide for experimental studies now underway.

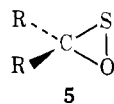
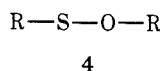
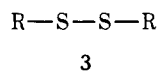
Current applications of quantum theory describe the interaction between lone electron pairs on adjacent atoms (**1**)



in terms of delocalized symmetric (n_+/π_+) and antisymmetric (n_-/π_-) combinations (Figure 1). The energy gap separating n_- and n_+ is a function of the magnitude of the interaction of the lone pair orbitals. For the simplest case, $\text{H}\ddot{\text{X}}\ddot{\text{X}}\text{H}$, ΔE is primarily dependent on the dihedral angle θ and the bond angle ϕ ($= \angle \text{XXH}$).

Experimentally the qualitative picture of Figure 1 has been substantiated by photoelectron spectroscopy (PES).³ Compound types as diverse as hydrazines,⁴ peroxides,⁵ disulfides,⁶ diphosphines,⁷ azoalkanes,⁸ and acetylenes⁹ conform to the predicted splitting pattern. Nonadjacent lone electron pairs behave similarly.¹⁰

In the present work we are concerned with the consequences of α -lone pair interaction when symmetry at the $\ddot{\text{X}}-\ddot{\text{X}}$ bond no longer prevails (**2**). The elimination of symmetry in systems capable of pericyclic transformation appears to alter significantly both the energetics¹¹ and the stereochemical course^{11b,12} of such reactions. By extension the conformational dynamics of **2** relative to **1** might be expected to reveal fundamental differences discernible within the framework of MO theory. For the present study CNDO calculations for the well-known disulfide moiety **3** are compared with those for the much less



investigated sulfenate ester unit **4**. This choice has been stimulated in part by our interest in the formation and reactivity of oxathiranes **5**.^{12a} There is ample evidence that the latter is probably an intermediate in both thermal and photochemical processes.¹³ Furthermore recent experiments are strongly suggestive that while **5** is but a transient at room temperature, certain derivatives can be trapped and observed directly at low temperature.¹⁴

Results and Discussion

Structure and Conformational Equilibria of RSSR and RSOR. A number of experimental and theoretical studies aimed at elucidating the potential energy surface for disulfides

have appeared.^{15–17} In order to test the reliability of CNDO/B as a predictor of both structural and orbital properties for this compound class, and by implication RSOR as well, we have studied the ground states and S–S rotational barriers for **3** (R = H, CH₃).

The structures of hydrogen persulfide (**3**, R = H) and dimethyl disulfide (**3**, R = CH₃) have been determined by microwave spectroscopy (cf. Table I). Using Boyd and Whitehead's CNDO parametrization,¹⁸ several sets of calculations have been carried out for these species. Table I lists the predicted structures for the cis, gauche, and trans conformations (0, 90, and 180°, respectively). Calculated bond lengths are in excellent agreement with experiment.¹⁹ However, the RSS bond angles are predicted to be 10–15° too large. The results of bond length optimization with fixed experimental RSS angles (Table I) also give highly satisfactory agreement with experiment. Dihedral angles for HSSH were optimized with excellent results leading to energy minima around 90°. For both staggered and eclipsed conformations of the CH₃ groups of dimethyl disulfide two calculations were carried out for each of the 0, 90, and 180° angles. For both methyl rotamers the gauche conformation is predicted to have the lowest relative energy.

The predicted barriers to rotation (Table I) in every case imply the trans barrier to be slightly less than or equal to the cis barrier. A variable temperature NMR study for a series of acyclic disulfides led to $\Delta H^\ddagger \leq 7$ kcal/mol for unhindered derivatives.²⁰ Remarkable is the conclusion, based on the effect of substituent bulk, that rotation most likely occurs preferentially through the cis conformation. This result has not yet been produced by theory, although the barrier problem has been taken up at all levels of sophistication ranging from extended Hückel to ab initio with extended basis sets (cis: 1.5–45.9 kcal/mol; trans: 0.8–14.5 kcal/mol).^{15–17} The cis/trans energy ratios previously reported and those indicated in Table I must be regarded with reservation. Minimum requirements for a reliable estimate of relative rotational barriers are an accurate prediction of ground-state geometry and RSS bending force constants followed by geometry optimization of the less stable rotamers.²¹ While CNDO/B is inadequately parametrized on the first count, previous calculations have ignored one or both of these points and have generally resorted to fixed and common geometries at all values of the dihedral angle. In the present study this problem has not been resolved. We note only that the CNDO/B results for HSSH are qualitatively similar to the ab initio work,¹⁷ but lead to lower barriers. For

Table I. CNDO/B Optimized Geometries for Conformers of HSSH and Staggered CH₃SSCH₃^a

R	θ (dihed), deg	r_{SS} , Å	r_{RS} , Å	$\angle SSR$, deg	Rel E , kcal/mol
H	0	2.052	1.333	108.8	1.7
		2.079	1.337	91.3	1.8
	88.7	2.043	1.336	107.9	0
	92.2	2.069	1.340	91.3	0
	(90.5) ^b	(2.055)	(1.327)	(91.3)	
	180	2.055	1.333	106.2	1.5
CH ₃	0	2.084	1.788	112.2	1.1
		2.115	1.811	102.8	5.5
	90	2.076	1.792	112.3	0
		2.100	1.807	102.8	0
	(84.7) ^c	(2.038)	(1.810)	(102.8)	
	(83.9) ^d	(2.022)	(1.806)	(104.1)	
	180	2.084	1.788	111.5	1.1
		2.106	1.811	102.8	4.0

^a The methyl groups were assumed to be tetrahedral and staggered¹⁹ with respect to the S-S bond. For all conformations $r_{CH} = 1.09$ Å. The first calculation listed for a given dihedral angle represents the fully optimized structure; the second utilized fixed bond angles (i.e., H, $\angle SSH = 91.3^\circ$; CH₃, $\angle SSC = 102.8^\circ$). Parenthetical values are experimental. ^b Reference 56. ^c Reference 19a. ^d Reference 19b.

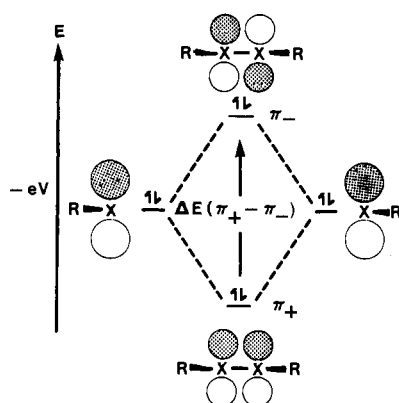


Figure 1. The interaction of identical, adjacent π -type lone electron pairs to give symmetric (π_+) and antisymmetric (π_-) delocalized molecular orbitals. The splitting, ΔE , is primarily due to the X-X distance and the RXXR dihedral angle.

CH₃SSCH₃ with the experimental CSS angle, our calculation reproduces measured disulfide barriers with a remarkable accuracy unmatched by other semiempirical schemes.

Finally a plot of CNDO/B eigenvalues (ϵ) surrounding the frontier orbital gap as a function of dihedral angle (θ) is depicted in Figure 2 for the HSSH cis to trans transformation. Orbital shapes are sketched for the latter conformational extremes. Except for minor differences in the relative energies of certain MO's between 0 and 180°, the orbital correlation diagram is essentially superimposable with that calculated by EH, CNDO/2, and ab initio methods.^{16a,b} The corresponding CH₃SSCH₃ plot is similar and likewise in qualitative agreement with the results of previous studies.^{6,15a-c,16}

We conclude our discussion of the overall dynamics of the disulfide moiety by noting that with fixed experimental RSS bond angles, every important structural characteristic is reproduced quantitatively. Furthermore, the energetic behavior of the computed MO's as a function of conformation about the S-S bond assures qualitative representation of UV transitions as well.¹⁶

While disulfides may be synthesized by a wide variety of methods, sulfenic acid esters (RSOR') have been generally prepared by the action of alcohols and alkoxides on sulfonyl halides.²² The reversibility of the reaction and the sensitivity of the sulfenates to hydrolysis and disproportionation²³ have

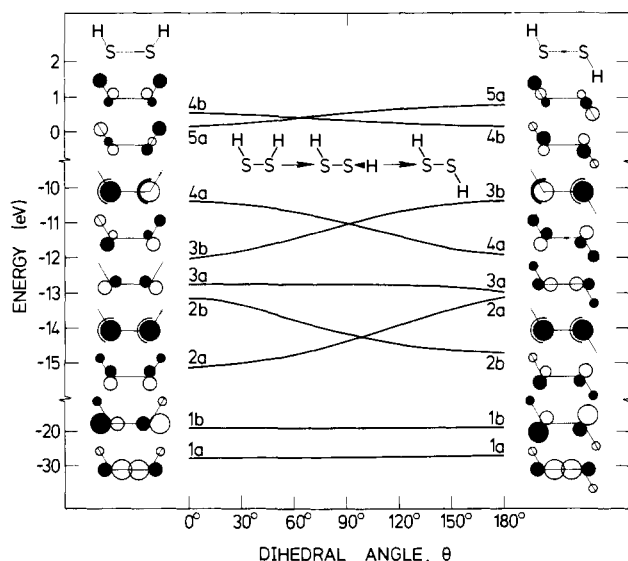
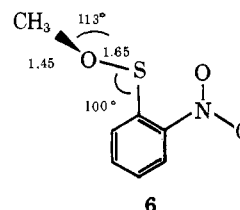


Figure 2. CNDO/B orbital correlation diagram for the interconversion of cis and trans forms of HSSH by rotation around the S-S bond. The shapes of the end point molecular orbitals (0 and 180°) are indicated by circles, the diameters of which are proportional to the square of the atomic orbital contributions at a given center. The MO's are labeled within the C₂ point group in accord with the dynamics of the cis/trans isomerization (cf. Figure 5).

limited the utility of the method by and large to aromatic derivatives.²⁴ A promising route employs *N-tert*-butylthiophthalimide as starting material for a series of *tert*-butylalkylsulfenates.^{22c,26} A single heavily-substituted cyclic case is known.²⁷ As yet, however, not only is the chemistry of the sulfenate function relatively undeveloped, but very little spectroscopic or structural information has been gathered. An exception is the *o*-nitrobenzenesulfenate (**6**), the x-ray struc-



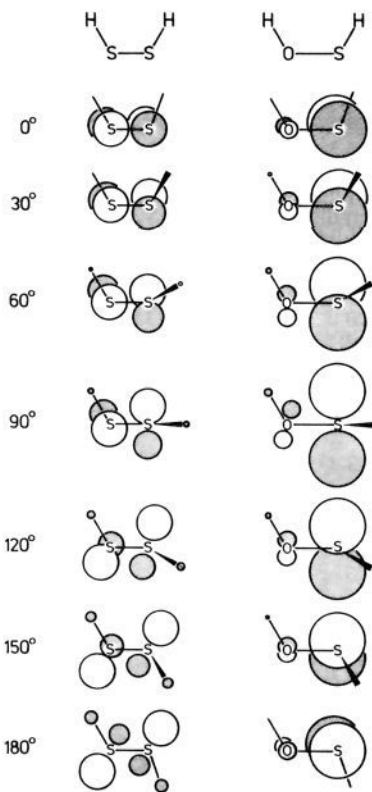


Figure 4. π^- HOMO population analysis for the stepwise transformation of HSSH and HSOH from the cis-planar to the trans-planar conformation. The circle diameters are proportional to the square of the contributing atomic orbital coefficients (CNDO/B).

correlation pictured in Figure 3. The situation arises because of the lack of molecular symmetry, which permits new bonding relationships across the potential energy surface for RSOR unavailable to the symmetric RSSR structure.

The basis for the orbital variations described above can be illuminated by considering the perturbations experienced by R-S bonded to a second S-R at various values of the dihedral angle. Figure 5a shows the energies of the p_S and n_S orbitals for a hypothetical *cis*-HSSH in which the α -lone pairs do not interact. The calculated energies were obtained by setting the lone pair resonance integrals ($\beta_{S_1S_2}$) to zero as prescribed by Baird.³¹ When lone pair-lone pair interaction is permitted, the π ($1b_1$ and $1a_2$) and n ($2a_1$ and $2b_2$) MO's are constituted as symmetric and antisymmetric pairs in the usual way (i.e., Figures 1 and 5b), π_+ falling below n_- . As rotation sets in, the orthogonality of the π and σ MO's in the planar disulfide is eliminated as HSSH symmetry is reduced from C_{2v} (*cis*) or C_{2h} (*trans*) to C_2 . Consequently the n_- and π_+ orbitals of b symmetry interact until a maximum separation is reached at the crossing point around 90° (Figure 5, $b \rightarrow c$). Concomitant with the changes in energy, n_- mixes-in π character while π_+ blends in σ character in accord with the well-established principles of perturbation theory.³²

A similar "repulsion" of the well-separated π_- and n_+ MO's of a symmetry is precluded by their great difference in energy. To a first approximation, however, rotation away from 0° reduces the overlap between AO components on adjacent sulfur atoms. Thus the antibonding and bonding character of π_- and n_+ is diminished, leading to a decrease and an increase in energy, respectively. Superimposed on these deformations are the energy-complementary alterations in MO composition described above in i and ii. The sum of the perturbations arising from the variation in mutual orientation of the R-S fragments gives rise to the double degeneracy around 90° depicted in

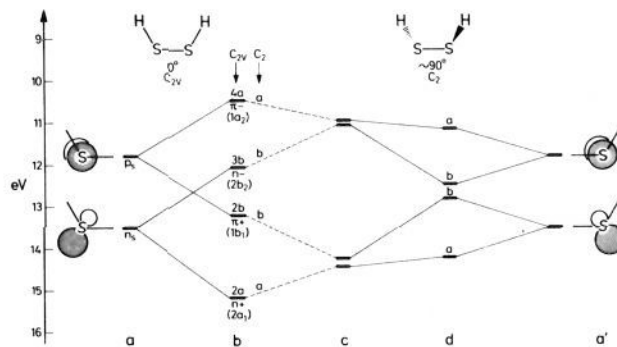


Figure 5. PMO analysis of the MO manifold for HSSH conformations: (a and a') the isolated lone pair components; (b) interaction of $p(S_1)/p(S_2)$ and $n(S_1)/n(S_2)$ in the *cis* (0°) conformation; (c) MO's for the *gauche* (90°) conformation; (d) interaction of the component p and n AO's in the *gauche* form.

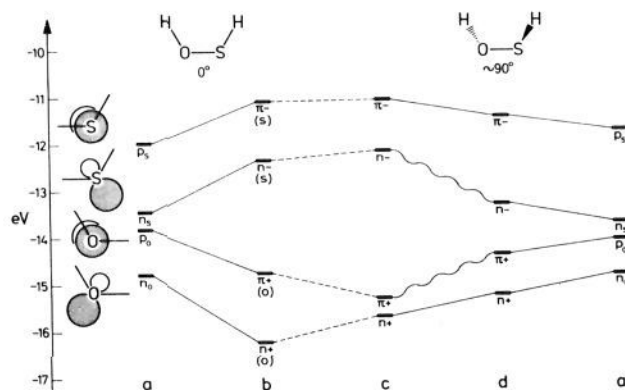


Figure 6. PMO analysis of the MO manifold for HSOH conformations: (a) a and a' are the isolated lone pair components; (b) interaction of $p(S)/p(O)$ and $n(S)/n(O)$ in the *cis* (0°) conformation; (c) MO's for the *gauche* (90°) conformation; (d) interaction of the component p and n AO's in the *gauche* form.

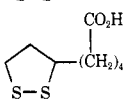
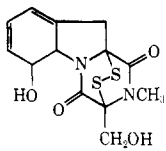
Figure 2. At this value of θ , π , σ and lone pair contributions are no longer distinguishable. We therefore label them simply n_p in the discussion to follow.

The same crossing-point result proceeds from the dissection of HSSH interactions in the *gauche* conformation. The hypothetically isolated lone pairs (Figure 5a') interact weakly because of unfavorable AO orientation to give the pair-wise level ordering shown in Figure 5d. Final interaction between MO's of symmetries a and b leads to the $\theta \approx 90^\circ$ result ($d \rightarrow c$).²⁹

The parallel analysis of rotation about the S-O bond in the sulfenate system is shown in Figure 6. Electronegativity differences between oxygen and sulfur are strongly reflected in the calculated ionization potentials for *cis*-HSOH in which the adjacent lone pairs are prevented from interacting ($\beta_{OS} = 0$, a). The complete calculation yields a level ordering (b) in which the high-lying MO's (π_- and n_-) are dominated by sulfur, while π_+ and n_+ are composed largely of contributions from oxygen (cf. Figure 3). As is the case for the disulfide moiety, n_- (S) lies above π_+ (O). However relative to HSSH, the energy gap has increased by over 100% from 1.1 to 2.4 eV. Consequently upon rotation through values $0^\circ < \theta < 90^\circ$, these MO's couple only weakly as shown in Figure 6, $b \rightarrow c$. The constancy of π_- (S) is rationalized by the opposite but balancing influences of less S-O π antibonding and the relatively effective mixing-in of σ OH character. The latter occurs in turn because the low-lying oxygen AO's are energetically well-disposed for blending with the hydrogen 1s species.

The construction of MO's for *gauche*-HSOH is shown on

Table III. Spectra (UV, PE), Geometries, and Predicted Dihedral Angles for Selected Disulfides

	IE ₁ , eV	IE ₁ -IE ₂ , eV (vertical)	Dihedral angle, θ , deg	Predicted θ based on Δ IE for staggered CH ₃ SSCH ₃			Bond angle, $\phi = \text{SSR}$, deg	λ_{max} , nm (ϵ)
				EH ^k	CNDO/S	CNDO/B		
HSSH	10.01 ^a	0.27	90.5 (MW) ^e	75-80		82	91.3 ^e	250 (370) ^l
CH ₃ SSCH ₃	8.98 ^b	0.24	84.7 (MW) ^f	80-83	81-82	74-77	102.8 ^f	250 (255) ^{m,n,o}
	9.00 ^d	0.25	83.9 (ED) ^g				104.1 ^g	
	9.01 ^c	0.27						
	8.97 ^a	0.30						259 (470) ^{o,p,q}
	8.36 ^a	0.95	60 (x-ray) ^h	62	60	41	99 ^h	290 (290) ^{o,r}
	8.02 ^d	1.80	35 (x-ray) ⁱ	16	33	0	92.7, 95.9 ⁱ	330 (160) ^{o,p,r}
			8.8, 15.8 (x-ray) ^j				97.9 (av) ^j	340 (200) ^s
<i>t</i> -BuSS- <i>t</i> -Bu	8.17 ^a	0.65		110	110	121		222 (460) ^{o,r,t}
	8.15 ^d	0.60						

^a Reference 6a. ^b Reference 6b. ^c Reference 6c. ^d Reference 6d. ^e Reference 56. ^f Reference 19a. ^g Reference 19b. ^h O. Foss, K. Johnson, and T. Reistad, *Acta Chem. Scand.*, 18, 2345 (1964). ⁱ I. L. Karle, J. A. Estlin, and K. Britts, *Acta Crystallogr.*, 22, 567 (1967); cf. O. Foss and O. Tjomsland, *Acta Chem. Scand.*, 12, 1810 (1958). ^j J. Fridrichsons and A. McL. Mathieson, *Acta Crystallogr.*, 23, 439 (1967). ^k Reference 16a. ^l F. Felner and H. Münzner, *Chem. Ber.*, 96, 1131 (1963). ^m Reference 47b. ⁿ Reference 38. ^o Reference 46a. ^p Reference 44. ^q V. Ramakrishnan, S. D. Thompson, and S. P. McGlynn, *Photochem. Photobiol.*, 4, 907 (1965). ^r References 45 and 46. ^s A. F. Beecham and A. McL. Mathieson, *Tetrahedron Lett.*, 3139 (1966). ^t C. W. N. Cumper, J. F. Read, and A. I. Vogel, *J. Chem. Soc. A*, 239 (1966).

the right side of Figure 6 ($a' \rightarrow d \rightarrow c$) and follows directly from the above discussion. The wavy lines indicate that π_- and π_+ are capable of interacting with both π_- and π_+ to give the final orbital set.

Photoelectron Spectra. The correlation diagram of Figure 2 in accord with previously reported MO diagrams^{6a,15a-c,16} qualitatively rationalizes a number of disulfide photoelectron spectroscopy (PES) studies.⁶ In all cases an unambiguous inverse relationship between Δ IE for the two lowest ionization potentials and θ is observed. The source of the Δ IE/ θ dependence and the regular increase of IE₁ with increasing θ (0-90°) has been attributed to the 3b-4a splitting pictured in Figure 2. By plotting Δ IE vs. the dihedral angle derived from microwave, electron diffraction, or x-ray determinations, a smooth curve is obtained which permits dihedral angles to be inferred from the PES spectra.^{6d} Unfortunately direct measurement of θ spans only the range 8-91° (cf. Table III). PES in conjunction with MO calculations has, however, been used to conclude that θ for *t*-BuSS-*t*-Bu is 97^{6b,33} and ca. 110°.^{6a} The former value is based on a simple MO model and agrees with an estimate from dipole moment data,³⁴ whereas the latter arises from an EH correlation diagram for CH₃SSCH₃. The corresponding angles from CNDO/S³⁵ and CNDO/B calculations of the potential energy surface for rotation about the S-S bond of dimethyl disulfide are 110 and 121°, respectively. Columns 4-6 in Table III indicate the relative abilities of these three semiempirical schemes to predict dialkyl disulfide dihedral angle from PES data. Although detailed structures are few, CNDO/S gives the most consistent quantitative result. Like all other semiempirical parametrizations, however, the first and second ionization potentials are overestimated^{16b} (10.8 and 11.0 eV, respectively; CH₃SSCH₃ ($\theta = 81^\circ$; CNDO/S, cf. Table III)).

No PES investigations have yet been reported for sulfenate esters **4**. Both CNDO/B and CNDO/S agree on two important points for these substances relative to disulfides. For an

increase in the dimethyl disulfide dihedral angle from 30 to 90°, the IE₁-IE₂ split is predicted to fall by 1.2 (CNDO/B) and 1.9 eV (CNDO/S). This is to be compared with ca. 1.5 eV derived experimentally (cf. Table III). The corresponding values for CH₃SOCH₃ are 0.1 and 0.7 eV, respectively. Secondly, whereas the first ionization potential (IE₁) for disulfides increases by ca. 1 eV for θ from 30 to 90°, both semiempirical parametrizations suggest a constant IE₁ for the SO rotamers (Δ IE₁ = 0.0 and 0.1 eV, respectively). Thus while the calculated values are probably somewhat low, IE₁ and IE₁-IE₂ are predicted to be much less sensitive to the dihedral angle for sulfenates than for disulfides in accord with the qualitative picture outlined in Figures 2 and 3. A recent measurement⁷ for the isoelectronic P-N bond of ((CH₃)₂N)₃P suggests that phosphorus-nitrogen interaction leads to a perturbation of the order of only 0.3-0.4 eV, in agreement with our speculations.

Ultraviolet Spectra. Boyd has tabulated disulfide derivatives in which θ varies from ~0 to ~125° and performed both an EHMO and a CNDO/2 analysis in the virtual orbital approximation, which accounts remarkably well for the dependence of the UV spectra on the dihedral angle.¹⁶ Within the EH model, for example, the two overlapping long-wavelength transitions (250 nm) for *gauche*-CH₃SSCH₃ and -HSSH have been interpreted as arising from excitation of the highest-lying filled MO's (4a, 3b; Figure 2) to the lowest virtual MO (4b); i.e., $n_p \rightarrow \sigma^*$ (H \rightarrow L and H-1 \rightarrow L).³⁶ As the dihedral angle is reduced from 90 to 0° the first transition is predicted to red shift and to lose intensity, in agreement with observation.

CNDO-CI calculations have likewise been carried out for HSSH^{15b,c} and CH₃SSCH₃.^{15c} Both EH and CNDO-CI^{15c} include sulfur 3d orbitals and suggest a high to predominant proportion of d character in the lowest energy virtual MO's. The SCF-CI treatment confirms the EH-generated conformational dependence of the first UV transition, but in addition provides a qualitatively more satisfying description for the

Table IV. Calculated Electronic Spectra of Dimethyl Disulfide as a Function of Dihedral Angle (λ_{\max} , nm); CNDO/S-CI^{a, b}

Dihedral angle, θ , deg						
0	30	60	90	120	150	180
306 (¹ B) H → L (0.96) H - 1 → L + 6 (0.03)	295 (¹ B) H → L (0.95) H - 1 → L + 6 (0.03)	276 (¹ B) H → L (0.93) H - 1 → L + 1 (0.03)	256 (¹ A) H → L (0.83) H - 1 → L + 2 (0.10)	279 (¹ A) H → L (0.93) H - 1 → L + 2 (0.03)	299 (¹ A) H → L (0.95) H - 1 → L + 2 (0.02)	309 (¹ A) H → L (0.95) H - 1 → L + 6 (0.03)
276 (¹ A) H → L + 1 (0.90) H - 1 → L + 2 (0.05)	267 (¹ A) H → L + 1 (0.88) H - 1 → L (0.05) H - 1 → L + 2 (0.04)	248 (¹ A) H → L + 1 (0.59) H - 1 → L (0.29) H - 1 → L + 2 (0.07)	255 (¹ B) H - 1 → L (0.82) H → L + 2 (0.11) H → L + 6 (0.04)	244 (¹ B) H - 1 → L (0.47) H → L + 2 (0.40) H → L + 5 (0.04)	248 (¹ A) H → L + 1 (0.89) H - 1 → L + 2 (0.06)	251 (¹ B) H → L + 2 (0.80) H - 1 → L (0.11) H - 1 → L + 1 (0.05)
232 (¹ B) H → L + 2 (0.75) H - 1 → L + 1 (0.21)	233 (¹ B) H → L + 2 (0.70) H - 1 → L + 1 (0.19) H → L + 3 (0.03)	232 (¹ B) H → L + 2 (0.71) H - 1 → L + 1 (0.21)	228 (¹ B) H - 1 → L + 1 (0.59) H → L + 2 (0.25) H - 1 → L (0.05) H → L + 6 (0.05)	240 (¹ A) H → L + 1 (0.84) H - 1 → L + 2 (0.10)	246 (¹ B) H → L + 2 (0.72) H - 1 → L (0.16) H - 1 → L + 1 (0.04)	247 (¹ A) H → L + 1 (0.87) H - 1 → L + 2 (0.08) H → L + 5 (0.04)
214 (¹ A) H - 1 → L (0.44) H → L + 6 (0.44) H → L + 4 (0.09)	215 (¹ A) H - 1 → L (0.53) H → L + 6 (0.35) H → L + 1 (0.03) H → L + 4 (0.03)	223 (¹ A) H - 1 → L (0.51) H → L + 1 (0.20) H - 1 → L + 2 (0.11) H → L + 6 (0.10) H → L + 5 (0.05)	227 (¹ A) H → L + 1 (0.60) H - 1 → L + 2 (0.25) H → L (0.06) H - 1 → L + 6 (0.05)	221 (¹ B) H - 1 → L + 1 (0.31) H - 1 → L (0.28) H → L + 2 (0.22) H → L + 6 (0.11)	215 (¹ B) H - 1 → L (0.38) H → L + 5 (0.30) H - 1 → L + 1 (0.11) H → L + 2 (0.09)	214 (¹ B) H → L + 6 (0.49) H - 1 → L (0.36) H - 1 → L + 1 (0.08) H → L + 2 (0.05)
200 (¹ B) H → L + 5 (0.89) H - 1 → L + 7 (0.09)	200 (¹ A) H → L + 4 (0.84) H - 1 → L + 2 (0.04)	194 (¹ A) H → L + 4 (0.45) H - 1 → L + 2 (0.23) H → L + 5 (0.10) H → L + 1 (0.09) H → L + 6 (0.04)	193 (¹ A) H - 1 → L + 2 (0.43) H → L + 1 (0.21) H → L + 3 (0.09) H → L + 8 (0.09) H - 1 → L + 5 (0.08) H - 1 → L + 9 (0.05)	194 (¹ B) H → L + 3 (0.40) H → L + 2 (0.20) H - 1 → L + 1 (0.14) H → L + 5 (0.09) H - 1 → L + 8 (0.09) H → L + 9 (0.03)	201 (¹ B) H → L + 3 (0.88) H - 1 → L + 8 (0.07)	200 (¹ A) H → L + 4 (0.91) H - 1 → L + 7 (0.09)

^aThe singlet transition symmetries (C_2) are indicated in parentheses after the λ_{\max} values; the CI state composition is to the right of the indicated excitation. For orbital nomenclature see ref. 36. ^bThe MO electron distributions for the 90° conformer are as follows: H - 1, H (S_p (88%)), L (S-S σ^* (39%)/3d (55%)), L + 1 (S-C σ^* (28%)/3d (69%)), L + 2 (S-C σ^* (25%)/3d (69%)), L + 3, L + 4, L + 5, L + 6 (3d (97-98%)). The percentage compositions change by no more than a few points from 0 to 180°.

Table V. Calculated Electronic Spectra of Dimethyl Sulfenate as a Function of Dihedral Angle (λ_{\max} , nm); CNDO/S—CI^{a, b}

		Dihedral Angle, θ , deg						
		0	30	60	90	120	150	180
329	H → L (0.99)	323	315	313	314	324	327	H → L (0.99)
244	H → L + 1 (0.98)	241	237	236	236	240	241	H → L + 1 (0.98)
194	H → L + 2 (0.99)	193	191	191	192	194	195	H → L + 2 (0.99)
186	H → L + 3 (0.99)	186	184	189	185	187	187	H → L + 3 (0.99)
		H → L + 3 (0.28)		H → L + 3 (0.26)				

^a The CI state composition is given in parentheses beneath each λ_{\max} ; for orbital nomenclature, see ref 36. ^b The MO electron distributions for the 90° conformer are as follows: H - 1 (S_p-O_p (20/58%)), H (S_p-O_p (89/3%)), L ($S-O \sigma^*$ (40%)/3d (56%)), L + 1 ($S-C \sigma^*$ (28%)/3d (68%)), L + 2, L + 3 (3d (99%)). The percentage compositions change by no more than a few points from 0 to 180°.

Table VI. The First UV Absorption Band for Comparable Acyclic Disulfides and Sulfenate Esters, λ_{\max} (ϵ)

	X	
	S	O
<i>t</i> -BuSXC ₂ H ₅	242 (450) ^{a, b}	266 (71) ^c
CCl ₃ SX- <i>t</i> -Bu	231 (2600) ^a	277 (390) ^d
CCl ₃ SXC ₂ H ₅	230 (2700) ^a	275 ^{c, e}
F ₃ CSXC ₂ H ₅	239 (269) ^f	262 (37) ^g

^a Reference 45. ^b Reference 46a and footnote *t* (Table III). ^c Reference 44. ^d R. S. Irwin and N. Kharasch, *J. Am. Chem. Soc.*, **82**, 2502 (1960). ^e Sample impurity prevented measurement of ϵ . ^f H. F. Emelús and S. N. Nabi, *J. Chem. Soc.*, 1103 (1960). ^g S. Andreades, *Chem. Abstr.*, **59**, 5024b (1963).

higher energy absorption bands. In particular the calculations of Richardson et al.^{15c} mimic circular dichroism studies which indicate the second transition (250 nm, $\theta \sim 90^\circ$) to blue shift from 90 to 60° and then red shift at still smaller angles. The short-wavelength absorption around 205–210 nm (90°) is characterized as a pair of overlapping bands of the $n_p \rightarrow S-R \sigma^*$ type with considerable admixture of the 3d's. Finally the intense high energy 196-nm transition (90°) is described as $S-S \sigma \rightarrow S-S \sigma^*$.³⁷

In order to consistently compare the disulfide and sulfenate ester functions, the conformational dependence of dimethyl derivatives has been investigated by the CNDO/S procedure.^{35b} This parametrization includes sulfur 3d orbitals and is designed specifically for the calculation of UV spectra of sulfur-containing compounds. Qualitatively the results for CH₃SSCH₃ (Table IV) agree in every essential detail with the Richardson et al. study.^{15c} The single exception is the fifth transition (196 nm, expt³⁸) which CNDO/S posits is $n_p \rightarrow S-C \sigma^*$. Quantitatively CNDO/S—CI is superior to all previously employed computational strategies in its ability to accurately reproduce experimental wavelengths without the expediency of scaling factors.

The calculated spectroscopic behavior of dimethyl sulfenate is presented in Table V. There are some significant differences between these results and those for dimethyl disulfide (Table IV). Firstly, in qualitative accord with the correlation diagrams of Figures 2 and 3, there is a very much less pronounced dependence of the longest wavelength band on the dihedral angle. Thus whereas CNDO/S predicts an increase of 50 nm (90° → 0°) for the $n_p \rightarrow \sigma^*$ (H → L) λ_{\max} of CH₃SSCH₃, the corresponding spread for CH₃SOCH₃ is only 16 nm. Secondly, the calculated spectrum for *gauche*-dimethyl sulfenate contains only a single excitation for the first absorption peak (313

nm) well separated from the next highest band. Thirdly, for any given dihedral angle, the sulfenate ester is predicted to show a lower energy long-wavelength transition relative to the disulfide. Finally the sulfenate transitions are nearly pure and thus simulated by single electron excitations (Table V). Analogous to CH₃SSCH₃ the first (313 nm) and second (236 nm) transitions for the *gauche* conformation correspond to $n_p \rightarrow S-O \sigma^*/3d$ and $n_p \rightarrow S-C \sigma^*/3d$ promotions, the 3d contribution amounting to 56 and 68%, respectively. The high-energy bands predicted at 191 and 189 nm are $n_p \rightarrow 3d$ and $n_p \rightarrow \sigma^*/3d$ (56%), respectively.

UV data for the sulfenate moiety is scarce. Some acyclic derivatives for which spectra have been reported are listed in Table VI. The λ_{\max} 's fall 20–50 nm below that calculated for the model dimethyl sulfenate cases. If the excellent agreement with experiment found for dimethyl disulfide carries over here, there may be two reasons for the discrepancy. The molecular structure of acyclic sulfenate esters is unknown. Thus we have been forced to take our geometric parameters for the calculations from the x-ray data of the half-aryl case **6**. More important, perhaps, two of the sulfenates in Table VI bear chlorine and fluorine atoms on carbon α to sulfur. Strongly electronegative substituents on disulfides are known to cause a hypsochromic shift. Bistrifluoromethyl disulfide, for example, exhibits its long-wavelength maximum at 237 nm (ϵ 360)³⁹ vs. 250 nm for CH₃SSCH₃ (Table III).

In spite of the paucity of data there are four sulfenate/disulfide pairs which can be compared (Table VI), and in all cases the former absorbs at lower energy. The comparison is not rigorously valid, since the shorter S—O bond might provoke steric repulsion between the R groups leading to opened dihedral angles. Nonetheless the agreement with theoretical prediction is striking and is indicative of the importance of employing a calculational procedure which includes CI—SCF when comparing the electronic spectra of symmetrical and unsymmetrical systems. In the present case reliance on the single configuration treatment would have led to the prediction that sulfenate esters ought to absorb at shorter λ_{\max} than disulfides.

The CNDO/S frontier orbital energy gap for $-S-O-$ is computed to be from 0.4 to 0.9 eV *greater* than for the corresponding $-S-S-$ for all structures considered in the present work. The single exception is CH₃SXCH₃ ($\theta = 90^\circ$) where the gap is identical for X = S and O. CNDO/B yields a similar result (cf. Figure 10). The source of the apparent discrepancy between $\Delta E(H-L)$ and the predicted spectra could lie in the CI treatment, which reduces the energies for lower excited states. The transition energies are thus calculated to be less than those estimated by considering only the MO's of the un-mixed ground-state configuration. Clearly the decrease af-

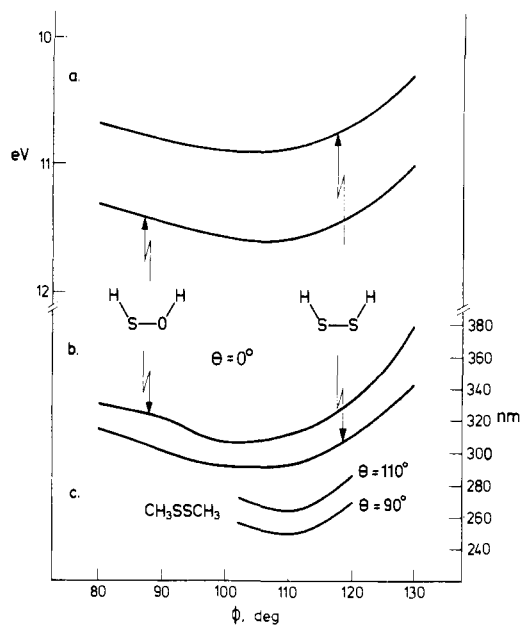


Figure 7. Calculated (CNDO/S) electronic variations of the RSXR system ($X = S, O$) as a function of the bond angle ϕ : (a) $\Delta E(\text{HOMO-LUMO})$ of planar HSXH; (b and c) the longest wavelength UV absorption for planar HSXH and CH_3SXCH_3 ($\theta = 90$ and 110°), respectively.

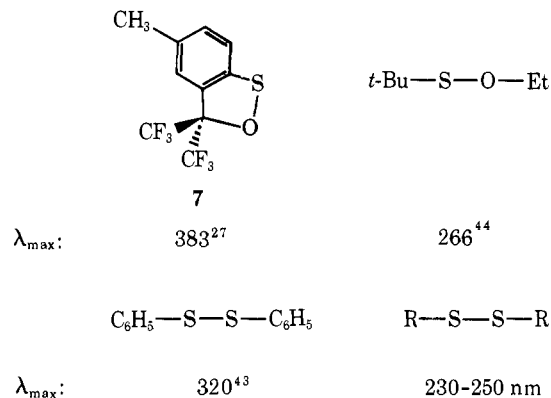
forded by CI is related to the extent of configuration mixing. Tables IV and V illustrate that improvement in the excited-state energies in this way is much more important for the disulfide system than for the sulfenate esters. The inclusion of CI, in fact, counters the computed SO/SS λ_{max} relationship.

An alternate source of the $\Delta E(\text{H-L})-\lambda_{\text{max}}$ dichotomy is found in expression 1 for the energy required to promote an electron from orbital k to the virtual orbital l via a singlet-singlet transition.^{35a,40} The symbols ϵ_k and ϵ_l are the energies of the initial and final orbitals, and J_{kl} and K_{kl} are the molecular Coulomb and exchange integrals.⁴¹

$$\Delta E = \epsilon_l - \epsilon_k - J_{kl} + 2K_{kl} \quad (1)$$

According to eq 1 the deviation of the transition energies from $\Delta E(\text{H-L})$ depends on the numerical values of the Coulomb and the exchange integrals. The latter are generally much smaller than the former and can to a first approximation be ignored.⁴² Thus we are led to the result that the low-energy, long-wavelength transition predicted and found for the sulfenate esters arises because of a sizable Coulomb integral, J_{kl} , relative to analogous disulfides. J_{kl} can be regarded as reflecting the mean repulsion between electrons occupying orbitals ψ_k and ψ_l . The MO's involved in the transitions in question are those which contain largely 3p and 3d components from sulfur and 2p contributions from oxygen. Since the latter are much less diffuse than the former, electron repulsion is expected to be greatest in the oxygen-substituted system; i.e., $J_{kl}(\text{SO}) > J_{kl}(\text{SS})$, implying $\Delta E(\text{SO}) < \Delta E(\text{SS})$. The magnitude of the repulsive effect must be considerable as it overrides both the $\Delta\Delta E(\text{H-L})$ and the CI factors.

The sulfenate dihedral angle dependence cannot be evaluated from experimental data at the present time. However, the cyclic sulfenate **7** has recently been prepared and exhibits a long-wavelength maximum at 383 nm (ϵ 70).²⁷ Since the compound incorporates $-\text{S}-\text{O}-$ in a five-membered ring, the weak low-energy transition offers a tempting analogy to the behavior of disulfides with reduced θ . It seems more likely, however, that the absorption of **7** is due to conjugation with the near coplanar phenyl group. A comparable bathochromic shift



is observed for diphenyl disulfide,⁴³ a conformationally flexible molecule, relative to acyclic disulfides.^{38,44-47}

The question of degenerate excitations for the sulfenate functionality is likewise still open. Comparison of the published spectrum of $t\text{-BuSOEt}$ ⁴⁴ with traces for both acyclic and cyclic disulfides^{38,44-46} indicates that although the sulfenate long-wavelength envelope (λ_{max} 266 nm) may possess a slightly narrower half-width than those recorded for RSSR, no definitive conclusion concerning the existence of overlapping bands can be drawn. In this connection Bergson has speculated on the appearance of two nondegenerate transitions for unsymmetrical molecules of type **2** at a dihedral angle of 90° .^{15a} However, based on theoretical arguments and a limited comparative UV study of disulfides, diselenides, and the mixed thioselenate system, RSSeR' , he and his coworkers^{45,48} concluded that there is no observable splitting of the first absorption band due to molecular asymmetry in any of the spectra and consequently no fundamental differences between the $-\text{S}-\text{S}-$, $-\text{S}-\text{Se}-$, and $-\text{Se}-\text{Se}-$ containing systems.⁴⁹ Although we have performed no calculations on the selenium derivatives, the first ionization potentials for the series R_2O , R_2S , and R_2Se ($\text{R} = \text{H}$:⁵⁰ 12.62, 10.47, and 9.93 eV; $\text{R} = \text{CH}_3$: 10.04,⁵¹ 8.67⁵¹/8.71,⁵² and 8.40⁵² eV, respectively) are consistent with Bergson's conclusions and the SS/SO comparisons of Figures 2 and 3. The large SO difference of 1.3-2.2 eV accounts for the interaction scheme of Figure 6. By contrast the 0.27-0.59 eV S/Se split is expected to lead to an RSSeR' correlation very similar to that predicted for disulfides.

The RSS and RSO/ROS Angles. In any series of $-\text{S}-\text{X}-$ ($X = S, O$) derivatives, the change in lone pair-lone pair interaction ought to be a function of both the dihedral angle θ and the RSX or R'XS bond angles ϕ . For small rings, in particular those containing three, four, and in some cases five members where the $-\text{S}-\text{X}-$ fragment is constrained to a common plane or nearly so, the bond angle ϕ might be dominant in determining changes in orbital energies as a function of ring size. Of equal interest, acyclic disulfides and sulfenates with bulky substituents might diminish steric strain by relaxing both ϕ and θ . In order to gain some insight into the effect of bond angle variation on UV spectra, model CNDO/S calculations for planar, *cis*-HSSH, and *cis*-HSOH have been performed for ϕ ranging from 80 to 130°. Both the frontier orbital energy gap and the first absorption band behave similarly. The curves of Figures 7a and b reveal "minima" at 103 and 106° for HSSH and HSOH, respectively. CNDO/B yields precisely the same result for the MO energy differences (Figures 8 and 9).⁶⁴

Thus ring contraction of hypothetical, planar disulfides and sulfenate esters is predicted to lead to red shifts in the UV. The overall result is in accord with measurements for cyclic disulfides. However for nonplanar RSSR' derivatives, both $\Delta\theta$ and $\Delta\phi$ influence the UV spectrum in the same direction. Furthermore the dihedral angle effect is clearly dominant. By reducing ϕ in HSSH from 105 to 90°, λ_{max} is predicted to increase by only 10 nm. Reduction of the dihedral angle from the

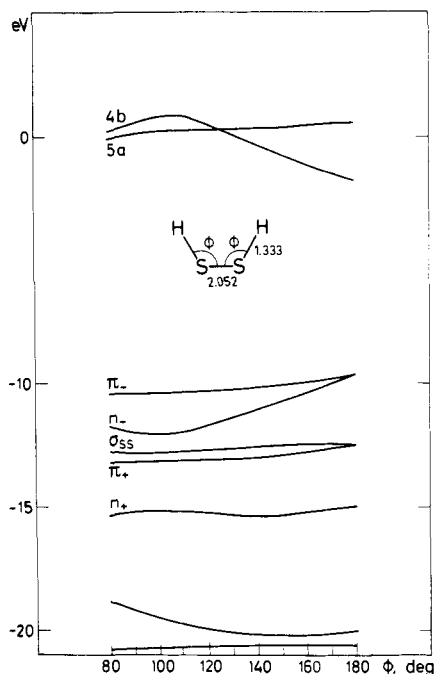
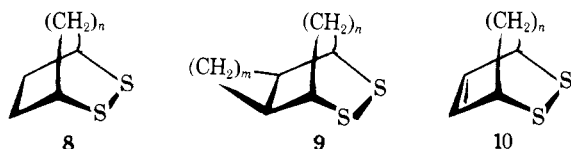


Figure 8. Molecular orbital correlation diagram for the expansion of the HSS bond angle of cis-planar HSSH from 80 to 180° (CNDO/B).

“gauche” value of 90° to that of the five-membered ring, 30°, leads to a calculated bathochromic shift for CH₃SSCH₃ of 40 nm. The problem of evaluating the relative influence of ϕ and θ is indicated in Table III. For every significant drop in ϕ , a much larger fall in θ obtains. Thus the effects of ϕ can be unambiguously distinguished from θ only by investigating a series of disulfides with a constant dihedral angle and a variable bond angle. In principle cis-bicyclic homologues such as **8**, **9**, and **10** might satisfy the criterion for $n = 1, 2, 3$ and $m = 1, 2$.⁵³ The compounds are, however, not yet available.



Although the known cyclic disulfides are incapable of providing information on the ϕ/θ problem, Table VII lists acyclic disulfide and diselenide series which may bear on the question. Thus homologous substitution of the -S-S- and -Se-Se- moieties leads to a hypsochromic shift of the first absorption band. Several workers have credited hyperconjugation as responsible.^{48a,54} The lack of an observable shift from HSSH to the methyl derivative, as well as the absence of a significant change from CH₃ to Et, reduces the plausibility of this proposal. Boyd^{16a} interpreted the spectra as reflecting an increase in dihedral angle with enhanced steric bulk. However, since the EH calculations predict a red shift for either increasing or decreasing θ relative to 90°, it was concluded that the disulfide bands listed in Table VII at <250 nm in fact represent the second transition, the first having been overlooked. The constancy of the extinction coefficients renders this explanation unlikely. Furthermore, it was precisely to avoid interpretative difficulties caused by overlapping of the higher energy excitations of disulfides with the first absorption band that prompted Bergson's study of the diselenides.^{45,48a} The long-wavelength maximum for the latter occurs in a region uncontaminated by other absorption, leaving little doubt as to the assignment of the first band in the -S-S- series.

A consistent interpretation of the hypsochromic shifts in-

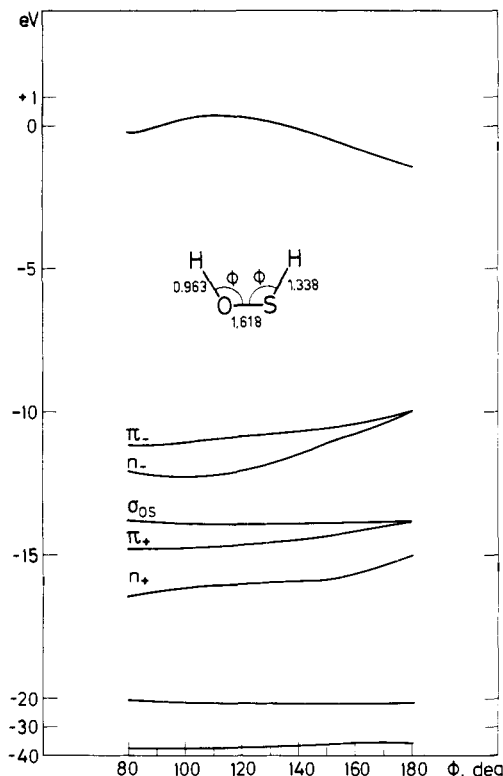


Figure 9. Molecular orbital correlation diagram for the expansion of the HSO and HOS bond angles of cis-planar HSOH from 80 to 180° (CNDO/B).

Table VII. The UV Spectra of Acyclic Dialkyl Disulfides and Diselenides as a Function of Substituent Bulk

R ₁	R ₂	λ_{\max} , nm (ϵ)	
		R ₁ SSR ₂	R ₁ SeSR ₂
H	H	250 (370) ^a	
CH ₃	CH ₃	250–255 (350) ^{b,c,d}	316 (310) ⁱ
Et	Et	249–252 (420) ^{b,e}	312 (420) ⁱ
Pr	Pr	250 (470) ^{f,g}	
Bu	Bu	252 (200) ^b	312 (380) ⁱ
<i>i</i> -Pr	<i>i</i> -Pr	245 (420) ^{d,g,f}	305 (420) ⁱ
<i>sec</i> -Bu	<i>sec</i> -Bu		305 (440) ⁱ
CH ₃	<i>t</i> -Bu	247 (410) ^h	
Et	<i>t</i> -Bu	243 (430) ^h	
<i>i</i> -Pr	<i>t</i> -Bu	240 (400) ^{d,h}	
<i>t</i> -Bu	<i>t</i> -Bu	222 (460) ^{d,g,h}	286 (460) ⁱ

^a Footnote *l* (Table III). ^b Reference 47b. ^c Reference 38. ^d Reference 46a. ^e Reference 47a. ^f Reference 44. ^g Footnote *t* (Table III). ^h Reference 45. ⁱ Reference 48a.

duced by homologation is that increasing steric bulk causes a relaxation of the SSC and SeSeC bond angles and perhaps the dihedral angle as well. In order to learn if the speculations evident from Figure 7a are general, the UV spectra of CH₃SSCH₃ have been calculated for fixed dihedral angles of 90 and 110° and variable SSC bond angles (102° → 120°); cf. Figure 7c. A small blue shift obtains with an increase in the SSC angle up to 110°. The order of magnitude of the calculated shift matches the observed displacement nicely.

The operation of a bond angle distortion of the type described cannot be unambiguously demonstrated at this time. Nonetheless the relative importance of angle bending vs. expansion of the dihedral angle for disulfides and diselenides is possibly indicated by the following. The potential barriers for rotation about the -O-O- bond in HOOH are 1.1 and 7.0

Table VIII. CNDO/B Optimized Geometries for Three- and Four-Membered Ring Disulfides and Sulfenate Esters^a (bond lengths, Å; bond angles, deg)

	X	r_{SX}	r_{SC}	r_{XC}	r_{CC}	r_{CH}	$\angle SCX$ (SCC)	$\angle XCS$ (XCC)	$\angle CSX$	$\angle SCH$	$\angle XCH$	$\angle HCH$
	11	S	2.103	1.795		1.094	71.7	71.7	54.1	118.7	118.7	107.3
	13	O	1.691	1.774	1.290	1.101	64.8	64.8	43.6	120.3	115.3	112.4
	12	S	2.146	1.835	1.564	1.105	99.1	99.1	80.9	114.2	114.2	104.6
	14	O	1.669	1.81 ^b	1.43 ^b	1.581 ^b	1.105 ^b	89.3	92.7	100.6	117.9	109.8

^a The planar four-membered rings are calculated to be more stable than puckered conformations. ^b Assumed values.

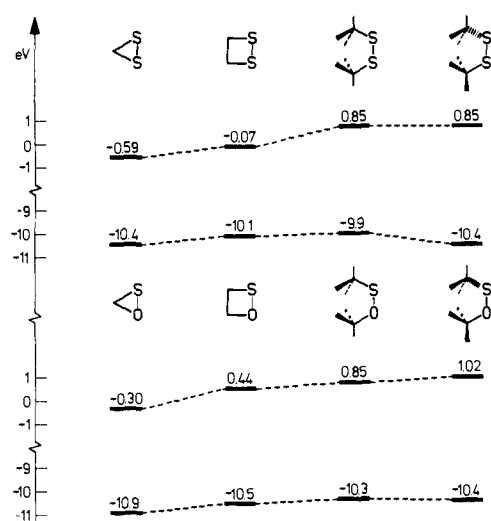
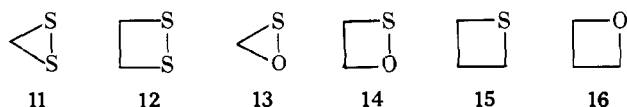


Figure 10. CNDO/B frontier orbital energies for selected disulfides and sulfenate esters. The dimethyl derivatives correspond to the *cis* and *gauche* staggered conformers, respectively. CNDO/S yields the same result qualitatively.

kcal/mol for the *trans* and *cis* pathways, respectively.⁵⁵ Microwave measurements⁵⁶ and *ab initio* calculations^{17b} lead to the conclusion that both HSSH barriers are considerably higher than the HOOH *cis* barrier. By contrast normal coordinate analysis⁵⁷ of CH_3OOCH_3 (ν_{COO} , sym = 448, antisym = 309 cm^{-1}), CH_3SSCH_3 (ν_{CSS} , sym = 240, antisym = 274 cm^{-1}), and $\text{CH}_3\text{SeSeCH}_3$ (ν_{CSeSe} , sym = 187, antisym = 193 cm^{-1}) evinces a reduction in the force constant for angle bending along this series.⁵⁸ Thus it appears as though XXC angle bending can compete more favorably with alterations in the dihedral angle as we progress from oxygen to sulfur to selenium. In the final analysis, a thorough evaluation of the hypsochromic shifts found in Table VII can be made only when the molecular structures of the bulky derivatives such as the *di-tert*-butyl cases are known.

Small Ring Geometries. In order to complete our analysis, we have optimized the geometries of the hypothetical three- and four-membered rings **11**–**14**. The resulting bond lengths and bond angles are given in Table VIII.



Of necessity the three-membered rings are planar. The CNDO/B parametrization predicts that both four-membered rings **12** and **14** are likewise flat. In the gas phase both thiethane⁶¹ (**15**) and oxetane⁶² (**16**) possess folded conformations interconverting through the planar form over an energy barrier of less than 1 kcal/mol. If capable of existence, **12** and **14** can

be expected to exhibit similar equilibrium behavior. The inability of a semiempirical calculation to discriminate faultlessly between conformations of vanishingly small energy differences is therefore not surprising.

Cis-Disulfides and Sulfenate Esters. The behavior of the frontier orbitals for the rings **11**–**14** and the *cis*-dimethyl RSXR derivatives are indicated in Figure 10. Several points emerge from the calculations. In agreement with the results for the HSXH species (Figure 7), a lower HOMO–LUMO energy gap with decreasing ring size (ϕ) is predicted for each series. Furthermore, for the small ring species the parallel with the acyclic models extends to the greater sulfenate $\Delta E(\text{HOMO}–\text{LUMO})$ compared to disulfides, the relative purity of disulfide/sulfenate UV transitions, and for the four-ring the red shifted $–\text{S}–\text{O}–$ first absorption band relative to $–\text{S}–\text{S}–$ (Table IX). The single exception to the inverse relationship between $\Delta E(\text{HOMO}–\text{LUMO})$ and the long-wavelength λ_{max} is the three-ring pair **11** and **13**. The latter oxathiirane is blue shifted by 26 nm relative to the hypothetical dithiirane **11**.

The predicted excitations for the small rings are essentially of the same type as found for the acyclic *gauche*-dimethyl derivatives. Differences arise as a result of the topology of the cycles. Since the structures are planar, two of the highest energy MO's are thus the symmetric and antisymmetric n_p combinations, π_+ and π_- (cf. Figures 1 and 11). The $\Delta E(\text{HOMO}–\text{LUMO})/\lambda_{\text{max}}$ reversal for **11** and **13** finds its origin here. Unlike dithiacyclobutane **12** and acyclic disulfide conformers, the π -type HOMO of the symmetric dithiirane **11** does not incorporate antibonding hydrocarbon fragment contributions. This translates into a calculated first absorption band that unlike all other $–\text{S}–\text{S}–$ derivatives treated by CNDO/S, but similar to the sulfenate esters, is nearly configurationally pure. The relative disulfide/sulfenate HOMO–LUMO energy gap in such a situation qualitatively reflects the calculated λ_{max} 's. Furthermore the three- and four-membered ring σ electrons are delocalized more extensively than in the acycles. The Walsh-type e_a , e_s , and e_u MO's^{32,63} are clearly evident. Nonetheless the first and second transitions can be catalogued as $n_\pi \rightarrow \text{S}–\text{X}$, $\text{S}–\text{C} \sigma^*$ (cf. Table IX) completely analogous to CH_3SXCH_3 . By comparison with the latter, however, the LUMO's contain somewhat less of a contribution from the sulfur 3d's (i.e. **11** (28%), **12** (45%), CH_3SSCH_3 (55%); **13** (36%), **14** (48%), CH_3SOCH_3 (56%)). This may be attributed to the more effective heavy-atom orbital mixing in the rings expressed by e_a^* and e_s^* .

An interesting feature of the π HOMO eigenfunctions is the finding that the oxathiirane **13** frontier orbital is best characterized as a nearly pure sulfur 3p orbital (87%) in contrast to the greater $p-\pi$ mixing found for the oxathiacyclobutane **14** (59% 3p) and *cis*- CH_3SOCH_3 (61% 3p). The CNDO/S parametrization yields a nearly identical set of AO coefficients. A possible cause is the CNDO/B result that the S–O bond length is longest in the three-membered ring.

The calculated first absorption band in the UV spectrum of

Table IX. Calculated Electronic Spectra for Three- and Four-Membered Ring Disulfides and Sulfonate Esters (λ_{\max} , nm); CNDO/S-CI^{a,b}

11	13	12	14
422 (¹ B ₁) H → L (0.97)	396 H → L (0.99)	346 (¹ B ₂) H → L (0.94) H - 1 → L + 1 (0.04)	368 H → L (0.98)
289 (¹ A ₂) H - 1 → L (0.53) H → L + 1 (0.45)	242 H → L + 1 (0.98)	276 (¹ A ₂) H → L + 1 (0.76) H - 1 → L (0.19) H - 1 → L + 2 (0.03)	234 H → L + 1 (0.98)
229 (¹ A ₂) H - 1 → L (0.37) H → L + 1 (0.45) H → L + 6 (0.11) H - 1 → L + 2 (0.70)	224 H - 2 → L (0.95)	224 (¹ B ₁) H → L + 2 (0.80) H - 1 → L + 1 (0.14)	192 H → L + 2 (0.98)
225 (¹ B ₁) H → L + 2 (0.82) H - 1 → L + 1 (0.13) H - 1 → L + 6 (0.05)	201 H - 1 → L (0.89) H - 1 → L + 1 (0.08)	213 (¹ A ₂) H - 1 → L (0.41) H → L + 6 (0.39)	
192 (¹ B ₂) H → L + 5 (0.68) H → L + 3 (0.21) H - 1 → L + 7 (0.10)	186 H → L + 2 (0.99)	196 (¹ B ₂) H → L + 4 (0.89) H - 1 → L + 7 (0.10)	

^a The singlet transition symmetries (C_{2v}) for **11** and **12** are given in parentheses after the λ_{\max} values; the CI state composition for all species is to the right of the indicated excitation. For orbital nomenclature see ref 36. ^b The MO electron distributions are as follows: **11**: H - 1, H (S-S π_s , π_a (88, 100%)), L (S-S and S-C σ^* (70%)/3d (28%), e_a^*), L + 1 (S-C σ^* (38%)/3d (58%), e_s^*), L + 2 (S-S and S-C σ^* (28%)/3d (72%), e_a^*), L + 3 to L + 7 (3d (97-100%)); **12**: H - 1, H (S-S π_s , π_a (95%)), L (S-S σ^* (50%)/3d (45%)), L + 1 (S-C σ^* (37%)/3d (60%), e_u^*), L + 2 (S-S and C-C σ^* (29%)/3d (68%)), L + 3 to L + 7 (3d (95-98%)); **13**: H - 2 (S-O π_s (8/61%)), H - 1 (S-O and S-C σ (56%)/O (18%)/C (23%)), e_a), H (S-O π_a (89/10%)), L (S-O, S-C, and O-C σ^* (63%)/3d (36%), e_a^*), L + 1 (S-C σ^* (34%)/3d (64%)), L + 2 (3d (99%)); **14**: H (S-O π_a (75/18%)), L (S-O and S-C σ^* (45%)/3d (48%)), L + 1 (S-C σ^* (18%)/3d (71%)), L + 2 (3d (99%)). The e_a , e_s , and e_u designations are indicated for orbitals of the Walsh-type.^{32,63}

13 (λ_{\max} 396 nm) arises from a single electron transition between the frontier orbitals (Table IX). Although it may be fortuitous, this transition is in remarkable accord with the 390-nm absorption recorded for a low-temperature, matrix-isolated species assigned the oxathiirane structure.¹⁴ Finally we note that the prominence of the sulfur 3p contribution to the HOMO of **13** has been implicated in an unusual orbital correlation for the ring closure to and rupture of oxathiiranes.^{12a}

Conclusion

RSSR and RSOR possess adjacent divalent lone pair atoms, exhibit comparable overall molecular geometries, and are predicted to undergo conformational transformation with qualitatively similar energy requirements. A more detailed comparison of both single configuration molecular orbitals and configuration mixing reveals that further resemblance, however, is superficial. The predicted differences should be discernible by techniques such as UV and photoelectron spectroscopy. The limited available data allowing a comparison of disulfide and sulfonate ester functions support the calculations, although more information is needed.

From a theoretical viewpoint the introduction of strong asymmetry into dynamic systems of all kinds can be expected to have similar consequences with the result that orbital correlations derived from symmetric models are generally not preserved. The deviations should be most easily detected in the conformational and mechanistic behavior of isoelectronic systems differing either in the type or in the position of hetero substitution.^{12a,c} Among the factors which could be singled out as a qualitative guide in this regard, the displacement of nodal surfaces in the high-lying MO's during molecular deformation may prove to be of utilitarian value.

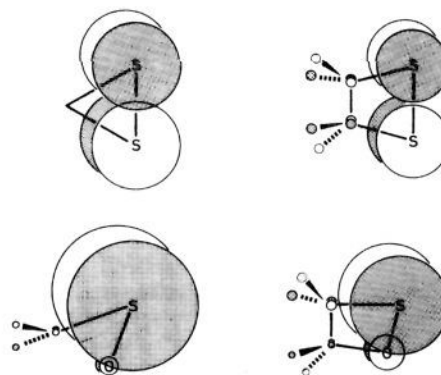


Figure 11. The π HOMO for cyclic disulfides **11** and **12** and cyclic sulfonate esters **13** and **14** (top view). Circle diameters are proportional to the square of the contributing atomic orbital coefficients.

Acknowledgment. We are grateful to the Danish Natural Science Research Council for generous financial support of the work and to Dr. B. Voigt (H. C. Ørsted Institute) for programming advice and several helpful discussions. Professor G. Pfister-Guillouzo (Université de Pau et des Pays de l'Adour) kindly provided a copy of CNDO/S. We are also appreciative to Dr. H. Johansen (the Technical University of Denmark) and D. B. Boyd (the Lilly Research Laboratories) for helpful comments.

References and Notes

- Organo-Sulfur Mechanisms. 5. For part 4, see L. Carlsen, A. Holm, E. Koch, J. P. Snyder, and B. Stilkerieg, *Tetrahedron*, in press; part 3, J. P. Snyder,

- J. Am. Chem. Soc.*, **96**, 5005 (1974).
- (2) Camille and Henry Dreyfus Teacher-Scholar Grant Recipient, 1971-1976.
- (3) Cf. (a) H. Bock and B. G. Ramsey, *Angew. Chem.*, **85**, 773 (1973); *Angew. Chem., Int. Ed. Engl.*, **12**, 734 (1973); (b) H. Bock and P. D. Mollère, *J. Chem. Educ.*, **51**, 506 (1974).
- (4) P. Rademacher, *Angew. Chem.*, **85**, 410 (1973); S. F. Nelsen and J. M. Buschek, *J. Am. Chem. Soc.*, **96**, 6987 (1974).
- (5) C. Batich and W. Adam, *Tetrahedron Lett.*, 1467 (1974).
- (6) (a) H. Bock and G. Wagner, *Angew. Chem.*, **84**, 119 (1972); G. Wagner and H. Bock, *Chem. Ber.*, **107**, 68 (1974); (b) A. D. Baker, M. Brisk, and M. Gellender, *J. Electron Spectrosc. Relat. Phenom.*, **3**, 227 (1974); (c) R. C. Colton and J. W. Rabalais, *ibid.*, **3**, 345 (1974); (d) M. F. Guimon, C. Guimon, and G. Pfister-Guillouzo, *Tetrahedron Lett.*, 441 (1975); M. F. Guimon, C. Guimon, F. Metras, and G. Pfister-Guillouzo, *Can. J. Chem.*, **54**, 146 (1976); *J. Am. Chem. Soc.*, **98**, 2078 (1976).
- (7) A. W. Cowley, M. J. S. Dewar, D. W. Goodman, and J. R. Schewiger, *J. Am. Chem. Soc.*, **95**, 6506 (1973); *ibid.*, **96**, 2648 (1974).
- (8) E. Haselbach and E. Heilbronner, *Helv. Chim. Acta*, **53**, 684 (1970); F. Brogli, W. Eberbach, E. Haselbach, E. Heilbronner, V. Hornung, and D. M. Lermal, *ibid.*, **56**, 1933 (1973); R. J. Boyd, J. C. Bünzli, J. P. Snyder, and M. L. Heyman, *J. Am. Chem. Soc.*, **95**, 6478 (1973); H. Schmidt, A. Schweig, B. M. Trost, H. B. Neubold, and P. H. Scudder, *ibid.*, **96**, 622 (1974); K. N. Houk, Y. M. Chang, and P. S. Engel, *ibid.*, **97**, 1824 (1975).
- (9) C. Batich, O. Ermer, E. Heilbronner, and J. Wiseman, *Angew. Chem., Int. Ed. Engl.*, **12**, 312 (1973); H. Schmidt, A. Schweig, and A. Krebs, *Tetrahedron Lett.*, 1471 (1974).
- (10) D. A. Sweigart and D. W. Turner, *J. Am. Chem. Soc.*, **94**, 5599 (1972).
- (11) (a) R. G. Pearson, *Top. Curr. Chem.*, **No. 41**, 99-102 (1973), and references cited therein; (b) N. D. Epiotis, *Angew. Chem., Int. Ed. Engl.*, **13**, 751 (1974).
- (12) (a) J. P. Snyder, *J. Am. Chem. Soc.*, **96**, 5005 (1974); (b) E. E. Weltin, *ibid.*, **96**, 3049 (1974); (c) B. Schilling and J. P. Snyder, *ibid.*, **97**, 4422 (1975).
- (13) W. F. Wilkens, Ph.D. Thesis, Cornell University, Ithaca, N.Y., 1961; *Cornell Univ., Agric. Exp. Stn., Mem.*, **No. 385**, 1 (1964); A. G. Schultz, C. D. de-Boer, and R. H. Schlessinger, *J. Am. Chem. Soc.*, **90**, 5314 (1968); R. H. Schlessinger and A. G. Schultz, *Tetrahedron Lett.*, 4573 (1969); J. Silhanek and M. Zbirovsky, *Chem. Commun.*, 878 (1969); B. Zwanenburg and J. Strating, *Q. Rep. Sulfur Chem.*, **5**, 79 (1970).
- (14) L. Carlsen, N. Harrit, and A. Holm, *J. Chem. Soc., Perkin Trans. 1*, 1404 (1976).
- (15) (a) G. Bergson, *Ark. Kemi*, **12**, 233 (1958); *ibid.*, **18**, 409 (1962); (b) J. Linderberg and J. Michl, *J. Am. Chem. Soc.*, **92**, 2619 (1970); (c) J. Webb, R. W. Strickland, and F. S. Richardson, *ibid.*, **95**, 4775 (1973); R. W. Strickland, J. Webb, and F. S. Richardson, *Biopolymers*, **13**, 1269 (1974); (d) H. Yamabe, H. Kato, and T. Yonezawa, *Bull. Chem. Soc. Jpn.*, **44**, 22 (1971); *ibid.*, 604 (1971); (e) D. Perahia and B. Pullman, *Biophys. Res. Commun.*, **43**, 65 (1971); R. W. Woody, *Tetrahedron*, **29**, 1273 (1973); H. E. Van Wart, L. L. Shipman, and H. A. Scheraga, *J. Phys. Chem.*, **78**, 1848 (1974).
- (16) (a) D. B. Boyd, *J. Am. Chem. Soc.*, **94**, 8799 (1972); (b) D. B. Boyd, *J. Phys. Chem.*, **78**, 1554 (1974); (c) D. B. Boyd, *Int. J. Quantum Chem., Quantum Biol. Symp.*, **No. 1**, 13 (1974).
- (17) (a) M. E. Schwartz, *J. Chem. Phys.*, **51**, 4182 (1969); I. H. Hillier, V. R. Saunders, and J. F. Wyatt, *Trans. Faraday Soc.*, **66**, 2665 (1970); (b) A. Veillard and J. Demuyneck, *Chem. Phys. Lett.*, **4**, 476 (1970).
- (18) R. J. Boyd and M. A. Whitehead, *J. Chem. Soc., Dalton Trans.*, 73, 78, 82 (1972).
- (19) (a) D. Sutter, H. Dreizler, and H. D. Rudolph, *Z. Naturforsch. A*, **20**, 1676 (1965); (b) B. Beagley and K. T. McAloon, *Trans. Faraday Soc.*, **67**, 3216 (1971).
- (20) R. R. Fraser, G. Boussard, J. K. Sanders, J. B. Lambert, and C. E. Mixan, *J. Am. Chem. Soc.*, **93**, 3822 (1971).
- (21) For discussions of the significance of geometry relaxation for dynamic systems see: I. R. Epstein and W. N. Lipscomb, *J. Am. Chem. Soc.*, **92**, 6094 (1970); A. Veillard, *Theor. Chim. Acta*, **18**, 21 (1970); J. M. Lehn and B. Munsch, *Mol. Phys.*, **54**, 521 (1971).
- (22) (a) L. Goodman and N. Kharasch, *J. Am. Chem. Soc.*, **77**, 6541 (1955); I. B. Douglas and D. A. Koop, *J. Org. Chem.*, **27**, 1398 (1962); (b) T. L. Moore and D. E. O'Connor, *Q. Rep. Sulfur Chem.*, **1**, 175 (1966); *J. Org. Chem.*, **31**, 3587 (1966); (c) D. H. R. Barton, D. P. Manly, and D. A. Widdowson, *J. Chem. Soc., Perkin Trans. 1*, 1568 (1975).
- (23) N. Kharasch, S. J. Potempa, and H. L. Wehrmeister, *Chem. Rev.*, **39**, 269 (1946).
- (24) Although a general method for preparing alkylmethyl sulfenate esters from methanesulfonyl chloride has been reported,^{22b} workers in other laboratories have not been able to reproduce the work to give uncontaminated RSOR' products.²⁵
- (25) D. N. Harpp (McGill University) and J. L. Kice (Texas Tech University); private communication.
- (26) (a) D. H. R. Barton, G. Page, and D. A. Widdowson, *Chem. Commun.*, 1466 (1970); (b) D. N. Harpp and A. Granata, unpublished work, private communication.
- (27) (a) G. W. Astrolages and J. C. Martin, *J. Am. Chem. Soc.*, **97**, 6909 (1975); (b) the Beer's law plot for sulfenate 7 is linear up to 0.016 M, ruling out the intervention of a dimer; ϵ 69.7; J. C. Martin, private communication.
- (28) W. C. Hamilton and S. J. Laplaca, *J. Am. Chem. Soc.*, **86**, 2289 (1964).
- (29) Correlation diagram details are dependent on the ordering of end point MO's. These in turn are a function of the basis set. At very small values of the dihedral angle, ab initio calculations invert the energies of n_- (3b) and π_+ (2b) relative to CNDO/B, giving π_+ (3b) and n_- (2b) (reported in ref 16b). As a result π_-/n_- (cis) correlates with n_+/n_- (trans) instead of n_+/π_- (trans) as shown in Figure 2. The textual analysis is not fundamentally altered by this difference. For example, arguments analogous to those depicted by Figure 5 can be constructed for the energy manifold derived from the larger basis sets.
- (30) (a) EH population analysis of the conformations of HSSH^{30b} suggests that the total electron density moves from sulfur to hydrogen as the molecule is twisted from 0 to 90°; (b) D. B. Boyd, *Theor. Chim. Acta*, **30**, 137 (1973).
- (31) N. C. Baird, *Theor. Chim. Acta*, **16**, 239 (1970).
- (32) Cf. R. Hoffmann, *Acc. Chem. Res.*, **4**, 1 (1971); W. L. Jorgensen and L. Salem, "The Organic Chemist's Book of Orbitals", Academic Press, New York, N.Y., 1973, pp 10-11; E. Heilbronner and H. Bock, "Das HMO-Modell und seine Anwendung," Verlag Chemie, GmbH, Weinheim, 1968; I. Fleming, "Frontier Orbitals and Organic Chemical Reactions," Wiley, New York, N.Y., 1976.
- (33) The 97° dihedral angle derived for t-BuSS-t-Bu^{6b} has been calculated by analyzing the measured differences in the two highest ionization potentials by means of Nelander's version³⁴ of Bergson's equation.^{48a} However the appearance of $|\cos \theta|$ does not assure a unique value of θ . For tert-butyl disulfide $\theta = 82^\circ$ is also permissible.
- (34) B. Nelander, *Acta Chem. Scand.*, **23**, 2127 (1969).
- (35) (a) J. Del Bene and H. H. Jaffe, *J. Chem. Phys.*, **48**, 1807 (1968); (b) C. Guimon, D. Gonbeau, and G. Pfister-Guillouzo, *Tetrahedron*, **29**, 3399, 3599 (1973); M. Arbelot, C. Guimon, D. Gonbeau, and G. Pfister-Guillouzo, *J. Mol. Struct.*, **20**, 487 (1974).
- (36) For simplicity H = HOMO (highest occupied MO) and L = LUMO (lowest unoccupied MO). H - 1, H - 2, ... refers to the next highest occupied and the second highest occupied MO's, respectively. Likewise L + 1, L + 2, ... designate the next lowest, second lowest, and so on virtual orbitals.
- (37) For a detailed, comparative discussion of theoretical calculations for the disulfide moiety and their correlation with experiment, see ref 16b.
- (38) S. D. Thompson, D. G. Carroll, F. Watson, M. O'Donnell, and S. P. McGlynn, *J. Chem. Phys.*, **45**, 1367 (1966).
- (39) R. N. Hazeldine and J. M. Kidd, *J. Chem. Soc.*, 3219 (1953).
- (40) C. C. J. Roothaan, *Rev. Mod. Phys.*, **23**, 69 (1951).
- (41) For a qualitative interpretation of the electron repulsion terms J_{kl} and K_{kl} see (a) M. J. S. Dewar, "The Molecular Orbital Theory of Organic Chemistry", McGraw-Hill, New York, N.Y., 1969, pp 61-64; (b) J. Michl and E. W. Thulstrup, *Tetrahedron*, **32**, 205 (1976).
- (42) H. F. Schaefer III, "The Electronic Structure of Atoms and Molecules", Addison-Wesley, Reading, Mass., 1972, p 11; cf., however, ref. 41b.
- (43) H. J. Backer and H. Kloosterziel, *Recl. Trav. Chim. Pays-Bas*, **73**, 129 (1954).
- (44) J. A. Barltrop, P. M. Hayes, and M. J. Calvin, *J. Am. Chem. Soc.*, **76**, 4348 (1954).
- (45) G. Bergson, F. Claesson, and L. Schotte, *Acta Chem. Scand.*, **16**, 1159 (1962).
- (46) (a) B. Nelander, *Acta Chem. Scand.*, **23**, 2136 (1969); (b) J. P. Casey and R. B. Martin, *J. Am. Chem. Soc.*, **94**, 6141 (1972).
- (47) (a) H. Ley and B. Arends, *Z. Phys. Chem., Abt. B*, **15**, 311 (1932); (b) G. R. A. Brandt, H. J. Emelèus, and R. N. Hazeldine, *J. Chem. Soc.*, 2549 (1952).
- (48) (a) G. Bergson, *Ark. Kemi*, **13**, 11 (1958); (b) G. Bergson and G. Nordström, *ibid.*, **17**, 569 (1961).
- (49) In fact, the Bergson-Boyd disulfide model requires a pair of nearly degenerate long-wavelength transitions for acyclic disulfides and diselenides ($\theta \sim 90^\circ$). Later investigations^{15b,38} recognized their presence under the ill-resolved broad band at 250 nm.
- (50) Cf. ref 3b and citations therein.
- (51) P. Mollère, H. Bock, G. Becker, and G. Fritz, *J. Organomet. Chem.*, **61**, 113, 127 (1973).
- (52) J. D. Scott, G. C. Causley, and B. R. Russell, *J. Chem. Phys.*, **59**, 6577 (1973).
- (53) For the influence of a four-membered ring on the geometry of the bicyclo[2.2.2]octane framework, cf. T. Ottersen, C. Rømming, and J. P. Snyder, *Acta Chem. Scand. B*, **30**, 407 (1976).
- (54) N. A. Rosenthal and G. Oster, *J. Am. Chem. Soc.*, **83**, 4445 (1961).
- (55) R. H. Hunt, R. A. Leacock, C. W. Peters, and K. T. Hecht, *J. Chem. Phys.*, **42**, 1931 (1965).
- (56) G. Winnewisser, M. Winnewisser, and W. Gordy, *J. Chem. Phys.*, **49**, 3465 (1968).
- (57) (a) S. G. Frankiss, *J. Mol. Struct.*, **3**, 89 (1969); (b) M. E. Butwill Bell and J. Laane, *Spectrochim. Acta. Part A*, **28**, 2239 (1972).
- (58) For dimethyl peroxide it has been shown that the O-O stretch is strongly coupled to the COO bending vibration.^{57b} Consequently the vibrational frequencies of XXC alone do not offer a quantitative measure of the ease of angle bending. Although the force constants for the -S-S- and -Se-Se- derivatives are not known, vibrational analysis for CH₂XCH₃ (X = O, S, Se) indicates that stretch-bend interactions are far less severe for the S/Se cases.⁵⁹
- (59) J. R. Atkinds and P. J. Hendra, *Spectrochim. Acta*, **22**, 2075 (1966); J. M. Freeman and T. Henshall, *J. Mol. Struct.*, **1**, 31 (1967); Y. Shiro, M. Ohsaku, M. Hayashi, and H. Murata, *Bull. Chem. Soc. Jpn.*, **43**, 609 (1970).
- (60) A. D. Walsh, *J. Chem. Soc.*, 2288 (1953).
- (61) D. O. Harris, H. W. Harrington, A. C. Luntz, and W. D. Gwinn, *J. Chem. Phys.*, **44**, 3467 (1966); K. Karakida and K. Kuchitsu, *Bull. Chem. Soc. Jpn.*, **48**, 1691 (1975).
- (62) S. I. Chan, T. R. Borgers, J. W. Russell, H. O. Strauss, and W. D. Gwinn, *J. Chem. Phys.*, **44**, 1103 (1966).
- (63) Cyclopropane: A. D. Walsh, *Nature (London)*, **159**, 712 (1947); *Trans. Faraday Soc.*, **45**, 179 (1949); H. Basch, M. B. Robin, N. A. Kuebler, C. Baker, and D. W. Turner, *J. Chem. Phys.*, **51**, 52 (1969); cyclobutane: L. Salem and J. S. Wright, *J. Am. Chem. Soc.*, **91**, 5947 (1969); R. Hoffmann and R. B. Davidson, *ibid.*, **93**, 5699 (1971).
- (64) The overall features or the correlation diagram for HSSH were anticipated by Walsh, although the rise of π_- with an increase in ϕ was not explicitly predicted: A. D. Walsh, *J. Chem. Soc.*, 2288 (1953).